



Adipose-derived stem cell exosomes promote tumor characterization and immunosuppressive microenvironment in breast cancer

Qin Zhu¹ · Yukun Cao¹ · Jiaqi Yuan¹ · Yu Hu¹

Received: 15 June 2023 / Accepted: 13 November 2023 / Published online: 31 January 2024
© The Author(s) 2024

Abstract

Adipose-derived stem cells (ASC) or autologous fat transplantation could be used to ameliorate breast cancer postoperative deformities. This study aims to explore the action of ASC and ASC-exosomes (ASC-exos) in breast cancer characterization and tumor microenvironment immunity, which provided a new method into the application of ASC-exos. ASC were extracted from human adipose tissue for the isolation and verification of ASC-exos. ASC-exos were co-cultured with CD4⁺T cells, CD14⁺ monocytes and MCF-7 cells, respectively. The tumor formation of nude mice was also constructed. Cell characterization was determined by CCK8, scratch assay, and Transwell. Hematoxylin–eosin (HE), immunohistochemistry (IHC) and immunofluorescence (IF) staining were used to observe the histopathology and protein expression. CD4⁺T cell and CD14⁺ monocytes differentiation was detected by flow cytometry. Western blot, qRT-PCR and RNAseq were used to detect the action of ASC-exos on gene and protein expression. CD4⁺T cells could take up ASC-exos. ASC-exos inhibited Th1 and Th17 differentiation and promoted Treg differentiation of CD4⁺T cells. ASC-exos inhibited M1 differentiation and promoted M2 differentiation of CD14⁺ monocytes. ASC-exos promoted the migration, proliferation, and invasion, while inhibited apoptosis of MCF-7 cells. ASC-exos promoted the tumor formation of breast cancer. The effect of ASC-exos on tumor microenvironment immunity was in accordance with the above in vitro results. TOX, CD4 and LYZ1 genes were upregulated, while Mettl7b and Serpinb2 genes were downregulated in ASC-exos group. Human T-cell leukemia virus 1 infection pathway was significantly enriched in ASC-exos. Thus, ASC-exos promoted breast cancer characterization and tumor microenvironment immunosuppression by regulating macrophage and T cell differentiation.

Keywords Adipose-stem cell · Exosomes · Breast cancer · T cell · Tumor microenvironment

Abbreviations

ASC	Adipose tissue-derived stem cells
ASC-exos	ASC-exosomes
HE	Hematoxylin–eosin
HBSS	Hank's balanced salt solution
IF	Immunofluorescence
RIPA	Radioimmunoprecipitation analysis

Introduction

Breast cancer is the most common malignancy worldwide and the leading cause of cancer death [1]. Tumor-infiltrating lymphocytes have emerged as a clinically relevant and highly repeatable biomarker that can influence breast cancer prognosis and therapeutic response [2]. Obesity is known to be linked to a higher risk of more aggressive breast cancer and reduced survival rates for patients [3, 4]. Primary human breast cancer affects the progression of breast tumors by invading surrounding fat and contacting adipose cells, inflammatory infiltration, and fibrous interstitium [5]. In vivo, deletion of the neutrophil specific gene ATGL or ATGL inhibitor altered neutrophil lipid profiles and lung metastasis of breast tumors in mice [6]. Therefore, we suspected that adipose-derived stem cell (ASC) may be mediators of malignant characterization in breast cancer, but their specific role remains unclear.

✉ Yu Hu
huyula99@163.com

¹ Department of General Surgery, Xiangya Hospital, Central South University, No. 87 Xiangya Road, Changsha 410008, Hunan, People's Republic of China

ASC or autologous fat transplantation could be used to improve breast tissue regeneration after hysterectomy or postoperative breast cancer deformities [7, 8]. To date, the potential for ASC to promote breast cancer growth and invasion found in basic science studies has indeed not been confirmed in clinical trials [9]. At present, some studies supported the effectiveness and safety of enriching ASC from the matrix vessels of adult adipose tissue [8, 9]. However, it was not known whether transplanted or resident ASCs increased the recurrence of cancer. As a key component of breast stroma, ASC played an important role in the breast cancer microenvironment [10]. Cross-talk between ASC and breast cancer cells were multilateral, and could occur either directly through intercellular contact or indirectly through secretory bodies released by ASC/MSC, which were considered to be major effectors of their supporting, angiogenic, and immunomodulatory functions [11]. Therefore, ASC derived exosomes (ASC-exos) was intermediates took part in the malignant phenotype of breast cancer, but their role remains unknown.

ASC-exos were known to be important components of ASC paracrine release and have a variety of biological activities [12]. ASC-mediated immune/inflammatory processes in the tumor microenvironment by releasing paracrine signaling factors alone or as a cellular extracellular vesicles (EVs, exosomes) [13]. Adipose MSCs inhibited the differentiation and proliferation of T cells and reduced the production of proinflammatory cytokine interferon γ (INF- γ) [14]. MSCs exosomes could also promote M2-type macrophages to secrete the anti-inflammatory cytokines [15]. In breast cancer models, there is a lack of systematic research on the role of ASC-exos in tumor cell differentiation of T cells and macrophages as well as the regulation of Th1/Treg balance. Therefore, this study systematically studied the effects of ASC and ASC-exos on T cells, macrophages, and breast cancer cells. The potential mechanism of ASC-exos on tumor growth was analyzed by RNAseq, which may add new insights to the application of ASC-exos.

Materials and methods

Extraction of ASC and identification of adipogenic differentiation

Human adipose tissue was provided by the Xiangya Hospital, Central South University for the extraction of ASC. In short, the adipose tissue was cut to paste and washed. The rinsed tissue was placed in a plate and added with collagenase (0.3 $\mu\text{g}/\text{mL}$, 0.075% type II collagenase). The tissues were then transferred to a flask with a pipette and placed in a 37 °C-water bath for 30 min, with oscillations every 5–10 min. After 30 min, the digestion of collagenase was

terminated by normal saline. After balance, supernatant and undigested fat were removed by centrifugation. DMEM containing fetal bovine serum (10%, FBS) was used to precipitate the suspended cells. The remaining red blood cells were dissolved with 0.16 mol/L ammonia chloride. The cell suspensions were filtered through 200 mesh copper mesh and centrifuged for 10 min (1200 r/min) to obtain mononuclear cells. The cells were added into the culture medium for count. Cell concentration was adjusted to 10^4 cells/mL based on the count results. Adipogenic and osteogenic differentiation ability of adipose-derived stem cell (ASC) could be identified by oil red and alizarin red staining after 12 days of culture. The expression of the CD73, CD90, CD44, CD34, and HLA-DR markers in ASC was detected by flow cytometry.

Isolation and identification of exosomes from ASC

The third generation of human ASCs were transferred to a centrifuge tube and centrifuged at 3000 g at 4 °C for 10 min to remove cell debris from the cell supernatant. To remove impurities, exosome concentration solution (ECS, UR52121, Umibio) was added to the centrifuge supernatant. For every 20 mL of sample, 5 mL of ECS reagent was added. The samples were mixed using a vortex oscillator and then placed at 2–8 °C for 2 h.

Afterward, the centrifuge tube containing the mixed liquid was taken out and centrifuged at 10,000 g at 4 °C for 60 min. The supernatant was discarded, and the precipitation was found to contain abundant exosome particles. To wash the centrifugal precipitate, 100 μL of $1 \times \text{PBS}$ was taken and evenly sprayed onto it. The suspension was then transferred to a 1.5-mL centrifuge tube and centrifuged at 4 °C at 12,000 g. This process helped to obtain the supernatant enriched with exosome particles.

The coarse exosome particles were carefully transferred into the upper chamber of the exosome purification filter (EPF column) and centrifuged at 3000 g at 4 °C for 10 min. After centrifugation, the liquid at the bottom of the EPF column (purified exosome particles) was collected. Finally, the exosomes were characterized using electron microscopy and particle size analysis. The expressions of CD9, CD63, and CD81, Tubulin and β -actin in the exosomes were tested using western blot.

Transmission electron microscopic observation of ASC-exo

The exosomes were resuspended in 100 μL of 2% PFA (P6148, SIGMA). Then, 5 μL of the exosome suspension was added to a formvar-carbon sample carrier copper mesh (01753-F, PELCO). Subsequently, 100 μL of PBS was added to the sealing film, and the copper mesh (with the Formvar

membrane facing down) was carefully placed on the PBS droplets using tweezers for cleaning purposes. Afterward, the copper mesh was placed in a 50- μ L droplet of 1% glutaraldehyde (16,051, Ted-pella) for 5 min. Following that, the copper mesh was cleaned by placing it in 100 μ L of ddH₂O₂ (E130-01A, Novoprotein) for 1 min. It was then transferred to a 50- μ L droplet of uranium oxalate dioxyoxide liquid for 5 min. After cleaning, the copper mesh was placed on 50 droplets of methyl cellulose for 10 min while kept on ice. Next, the copper mesh was positioned in a stain-less steel ring, and any excess liquid was absorbed and allowed to dry. Finally, the copper mesh was placed in a box and imaged under an electron microscope (1230, JEOL) at 80 kV.

Exosomes uptake test

Exosomes were resuspended with 1 ml PBS. PKH67 reagent (2 μ L) was added and incubated at 37 °C for 20 min to label exosomes. Serum (10 μ L) was added to terminate the reaction. Labeled exosomes (100 μ L) were added to the climbing sheets to cover the cells. Then, cells climbing sheets were incubated at 37 °C for 30 min–1 h and washed with PBS. DAPI (1 mg/mL) was added to cells climbing sheets and incubated, which were observed and photographed under fluorescence microscope (BA210T, Motic).

Cell experiment and grouping

The ASC-exos [16, 17] were divided into Control group, 1 μ g/mL group, 5 μ g/mL group, and 10 μ g/mL group. ASC-exos were co-culture with 2×10^5 CD4⁺T cell for 6 days to analyze the differentiation [14]. ASC-exos were co-culture with 2×10^5 CD14⁺ monocytes for 30 h to analyze the M1/M2 phenotype [18]. ASC-exos were co-culture with 5×10^6 MCF-7 cells (AW-CCH139, Abiowell) for 2 days to detect cell characterization.

The separation of CD14⁺ monocytes from human peripheral blood was performed as follows. LymphoPrep (#07811, Axis-Shield) was used to purify cells by density gradient centrifugation. CD14 MicroBeads (human, 130-050-201, Miltenyi) was applied to sort CD14⁺ monocytes. CD14⁺ monocytes were cultured in RPMI 1640 medium.

CD4⁺T cells were sorted by kit. The separation of CD4⁺T cells from human peripheral blood was performed by EasySep™ Human CD4⁺T Cell Isolation Kit (17,952, STEMCELL Technologies).

The study was approved by the Human Research Ethics Committee of Xiangya Hospital, Central South University (AF/SQ 2022090918). The research was conducted according to the World Medical Association Declaration of Helsinki. All the information about the study will be fully explained to the subjects by the researchers. All the participants provided informed consent before sampling.

Tumorigenesis in nude mice

A total of 10 BALB/c mice (22–28 g, 6–8 weeks) were bought from Hunan Slake Jingda Experimental Animal Co., Ltd. The log-growing MCF cells were centrifuged at room temperature at $500 \times g$, washed with Hank's balanced salt solution (HBSS) and re-suspended with 50% Matrigel (BD Biosciences). Cell suspension (100 μ L) was injected subcutaneously near the adipose pad of the fourth breast at a concentration of 5×10^5 cells/mL [19]. Mice were divided into Control group (PBS) and Exosome group (ASC-exos, 60 μ g/100 μ L), 5 mice/group. Mice in exosome group was given ASC-exos by the tail vein injection once a day for seven days and then every three days for a total of 28 days [20]. The control group was given equal volume PBS. The tumor was measured weekly using a caliper for the calculation of tumor volume by the modified ellipsoid formula $1/2 \times (\text{length} \times \text{width}^2)$. This study was approved by the Animal Ethics Committee of Xiangya Hospital, Central South University (AF/SQ 2022090918). All experimental procedures were conducted in accordance with institutional guidelines for the use of experimental animals.

Cell counting kit-8 (CCK8)

The cells were counted and then inoculated into a 96-well plate (100 μ L per well) with a density of 5×10^3 cells/well. After culture adherent, 100 μ L CCK8 solution (10:1, NU679, DOJINDO) was added. The cells were incubated and then detected by the Bio-Tek assay (MB-530, HEALES).

Scratch test

The horizontal lines were drawn by marker behind the 6-hole plate (3516, Corning). After counting, about 5×10^5 cells/well were added. Once the plate was covered with cells, the gun was crossed perpendicular to the line drawn before. The cells were washed with sterile PBS for 3 times. The scratched cells were removed and added serum-free DMEM medium (D5796, Sigma). The scratches were photographed under a microscope (DSZ2000X, Cnmicro) at the 0-h time point, and three different fields of view were captured. After culture for 24 and 48 h, photos were taken again.

Transwell

The lower part of the chamber (3428, Corning) was supplemented with 500 μ L 10% Gibco fetal bovine serum complete medium. Cells (2×10^6 cells/mL, 100 μ L) were add to each well and incubated at 37 °C for 48 h. The upper chamber was removed and placed into a new hole with PBS, which was washed 3 times. The upper chamber was fixed

with 4% paraformaldehyde for 20 min to obtain the membrane. The membrane was stained with 0.1% crystal violet (G1062, Solarbio) for 5 min and washed. The membrane was placed on the slide to observe cells under an inverted microscope. The chamber was removed and added to 500 μ L and soaked with 10% acetic acid for decolorization. At 550 nm, the absorbance value was measured by Bio-Tek assay (MB-530, HEALES).

Hematoxylin–eosin (HE) staining

Tumor tissue sections were roasted. Sections were dewaxed to water by using xylene and gradient ethanol. Sections were stained with hematoxylin (Abiowell) and eosin (Abiowell), respectively. Sections were observed by a microscope (BA210T, Motic).

Immunohistochemistry (IHC)

The tumor tissue sections were immersed in 0.01 M citrate buffer (pH 6.0), heated in a microwave until boiling, and then turned off. They were boiled continuously for 20 min. After cooling for 20 min, the slices were taken out and brought to room temperature. After cooling, the slices were washed with 0.01 M PBS (pH=7.2–7.6) for 3 min \times 3 times. The slices were then added to 1% high iodine acid at room temperature for 10 min to inactivate endogenous enzymes. They were washed with PBS for 3 min \times 3 times. The slices were incubated with appropriately diluted anti-Ki67 (1:200, ab16667, abcam, UK) overnight at 4 °C. Then, 100 μ L of anti-IgG (H+L, SA00013-2, Proteintech, USA) was added to the slices and incubated at 37 °C for 30 min. Next, 50–100 μ L of pre-made DAB working solution was added to the slices and incubated at room temperature for 1–5 min, followed by rinsing with distilled water. The slices were counterstained with hematoxylin for 5–10 min, washed with distilled water, and then returned to blue with PBS. The slices were dehydrated with graded ethanol (60–100%) for 5 min at each step. The slices were placed in xylene for 10 min \times twice. Finally, the slices were mounted with neutral gum and observed under a microscope (BA210T, Motic).

Immunofluorescence (IF)

According to the above steps, tumor tissue sections were subjected to antigen retrieval. Afterward, the sections were placed in a sodium borohydride solution at room temperature for 30 min, followed by rinsing with tap water for 5 min. The sections were then immersed in a 75% ethanol solution for 1 min. Subsequently, the sections were placed in a Sudan Black staining solution at room temperature for 15 min,

followed by rinsing with tap water for 5 min. The sections were blocked with 15% BSA for 60 min. Tissue sections were dripped with appropriately diluted primary anti-FoxP3 (1:100, PA5-85,236, ThermoFisher, USA) at 4 °C overnight. Then, it was incubated with 100 μ L coraLite488 conjugated affiniPure goat anti-Rabbit IgG (H+L, SA00013-2, Proteintech, USA). The sections were stained with DAPI working solution at 37 °C for 20 min, followed by PBS rinsing for 5 min, repeated 3 times. The sections were mounted with buffered glycerol and observed under a fluorescence microscope (BA210T, Motic).

Flow cytometry

The expression of the CD73, CD90, CD44, CD34, and HLA-DR markers in ASC was detected by flow cytometry. In brief, ASC was added and incubated with anti-CD73 (11-0739-42, eBiosciences), anti-CD90 (11-0909-42, eBiosciences), anti-CD44 (11-0441-82, eBiosciences), anti-CD34 (11-0349-42, eBiosciences), and anti-HLA-DR (11-9956-42, eBiosciences) for staining at room temperature for 30 min away from light, respectively. At the same time, the non-dye tube was set. Then, cells were washed by 1 mL PBS and analyzed by flow cytometer (A00-1-1102, Beckman).

To explore the phenotype changes of macrophages, $1 \times 10^6/100 \mu$ L cells were added into the centrifuge tube for PBS washing and centrifugation to remove the supernatant. The 0.125 μ g anti-CD206 (MA5-23,656, eBiosciences), 0.125 μ g anti-CD68 (11-0689-42, eBiosciences), and 0.5 μ g anti-CD8 (11-0081-82, eBiosciences) were added to each tube for staining at room temperature for 30 min away from light. Then, cells were washed by 1 mL PBS and analyzed by flow cytometer (A00-1-1102, Beckman). In addition, cells were examined for apoptosis by the annexin V-APC apoptosis detection kit (KGA1022, KeyGEN BioTECH).

To explore the differentiation of CD4⁺T cells, 1×10^6 cells (100 μ L) were added to 1.5 mL EP tubes with plus protein transport inhibitors (500 \times , 00-4975-93, eBiosciences) for incubation 4 h. Cell precipitate was suspended with Fixation/Permeabilization concentrate (500 μ L, 1 \times , 00-5123-43, eBiosciences) and fixed at room temperature for 30 min away from light. Permeabilization Buffer (1 mL, 1 \times) was added to the cell precipitation. The cells were suspended, centrifuged, and added 100 μ L PBS. Each tube was added with 0.25 μ g anti-CD4 (11-0041-82, eBiosciences) and 0.25 μ g anti-IL-17A (12-7179-42, eBiosciences) to detect Th17 cells. Each tube was added with 0.25 μ g anti-CD4 (11-0041-82, eBiosciences), 0.25 μ g anti-CD25 (12-0250-42, eBiosciences), and 1 μ g anti-Foxp3 (17-5773-82, eBiosciences) to detect Treg cells. Each tube was added with 0.25 μ g anti-CD4 (11-0041-82, eBiosciences) and 0.25 μ g anti-IFN- γ (12-7311-82, eBiosciences) to detect Th1 cells. The cells were incubated and tested by flow cytometry (A00-1-1102, Beckman).

Quantitative reverse transcription-PCR (qRT-PCR)

Total RNA was extracted by Trizol (15,596,026, Thermo). Using total mRNA as template, cDNA was synthesized by the mRNA (CW2569, cwbiotech) kit. The target genes (Table 1) were detected by UltraSYBR Mixture (CW2601, cwbiotech) on the RCP instrument (PIKOREAL96, Thermo). β -actin and GAPDH were used as internal parameters. The $2^{-\Delta\Delta C_t}$ algorithm was applied to calculate the expression of target genes.

Western blot

The proteins in cells and tissues samples were extracted by the radioimmunoprecipitation analysis (RIPA) and lysis buffer. The protein concentration was determined by bicinchoninic acid. Protein samples were isolated by 12% SDS-PAGE. The isolated proteins were transferred to a polyvinylidene fluoride film activated by methanol and sealed with 5% skim milk and dried at room temperature for at least 1 h. The membrane was then incubated with the first antibody overnight at 4 °C, which included anti-CD63 (25682-1-AP, 1:300, Proteintech, USA), anti-CD81 (66866-1-Ig, 1:3000, Proteintech, USA), anti-CD9 (20597-1-AP, 1:600, Proteintech, USA), anti-Tubulin (11224-1-AP, 1:3000, Proteintech, USA), anti-Bax (50599-1-AP, 1:6000, Proteintech, USA), anti-Bcl-2 (12789-1-AP, 1:2000, Proteintech, USA), anti-ERBB2 (#2165, 1:1000, CST, USA), anti-Ki67 (ab16667, 1:1000, abcam, UK), anti-Arg-1 (16001-1-AP, 1:20,000, Proteintech, USA), anti-CD163 (16646-1-AP, 1:600, Proteintech, USA), anti-TNF- α (17590-1-AP, 1:600, Proteintech, USA), anti-iNOS (18985-1-AP, 1:600, Proteintech, USA), anti- β -actin(66009-1-Ig, 1:5000, Proteintech, USA), and GAPDH (10494-1-AP, 1:5000, Proteintech, USA). Then, it was incubated with anti-IgG (SA00001-1, 1:5000; SA00001-2, 1:6000, Proteintech, USA). Visualization and imaging analysis were performed by GE Healthcare software (Life Sciences, USA).

RNAseq

RNA extraction and library construction were performed in tumor tissues. Illumina PE150 was applied for on-machine sequencing to collect the raw data. Fastp (<https://github.com/OpenGene/fastp>) was used for quality control to obtain the clean reads. HISAT2 was used to compare the filtered clean data with the reference genome sequence to obtain the reference genome. The stringtie software was used to reconstruct the transcript, assemble the exact transcript results, and count the expression of each gene or transcript. DESeq2 or edgeR were used to analyze the difference in expression level with or without biological duplication. Lastly, the Gene Ontology (GO, <http://www.geneontology.org/>) and KEGG

Table 1 Primer sequence

Gene	Primer sequence	Length (bp)
H-PPAR- γ	F TGCTCCAGAAAATGACAGACC R ATTTTCCTCAGAATAGTGCAAC	194
H-HSL	F CACTTAGCCCCTCCACACCCTT R TCAGCCTCTTCCCCTGCATCCTC C	70
H-LPL	F CAATCACAGCAGCAAAACCTT R GCCAGTCCACCACAATGACA	134
H-FABP4	F GGGCCAGGAATTTGACGAAG R AACTCTCGTGGAAAGTGACGC	184
H-ADIPOQ	F CATGACCAGGAAACCACGACT R ACCGATGTCTCCCTTAGGACCA	198
H-FoxP3	F CGCCACAACCTGAGTCTGC R CTCCAGCTCATCCACGGTCCA	81
H-IL-17-	F CAGATTACTACAACCGATCCACC R ACTTTGCTCCAGATCACA	90
H-IFN- γ	F AGAATGGCTGTGCTGACT R ATAGCTCTTCGGATACCTC	205
H-Arg-1	F TGGACAGACTAGGAATTGGCA R CCAGTCCGTCAACATCAAAACTA	102
H-iNOS	F TCAGCTGTGCCTTCAACCC R CCGAGGCCAAACACAGCGTA	199
H-TNF- α	F GAACCCCGAGTGACAAGCCT R TATCTCTCAGCTCCACGCCAT	120
H-CD163	F AAAAGAATCCCGCATTTGGCAGT	184
M-TOX	F GCTCCTCGCACAGAGATCAA R TTTCTTTTCTCCTGCCCGCT	167
M-CD4	F TTCTGGAAGTGCACCGTGACC R TCTCTGCCTTCCACATCAGC	184
M-LYZ1	F TCAGGAGGACTAGTGAGCTGT R CCTGTGGTTATTGGCTGGTACA	101
M-CSF3	F GTATAAAGGCCCCCTGGAGCTG R TGCAGGGCCATTAGCTTCAT	114
M-Mettl7b	F CATTACCCACTCTGTCCCCG R GGCTGCTTTATTGAGTGCCG	85
M-Serpinb2	F ATTTCTGTGTGTCAGCCGC R CCAGCACCGAGGAGAACTAT	184
M-Tbc1d2	F TCCTGTGCCCTGTGAAAACA R GTGCCCAGATGCTTTAGGGA	112
M-GAPDH	F GCGACTTCAACAGCAACTCCC R CACCCTGTTGCTGTAGCCGTA	122
H-actin	F ACCCTGAAGTACCCCATCGAG R AGCACAGCCTGGATAGCAAC	224
H-GAPDH	F ACAGCCTCAAGATCATCAGC R GGTCATGAGTCCCTTCCACGAT	104

(<https://www.kegg.jp/>) enrichment analysis was employed to identify pathways exhibiting significant enrichment in differentially expressed genes as compared to the entire reference transcriptome.

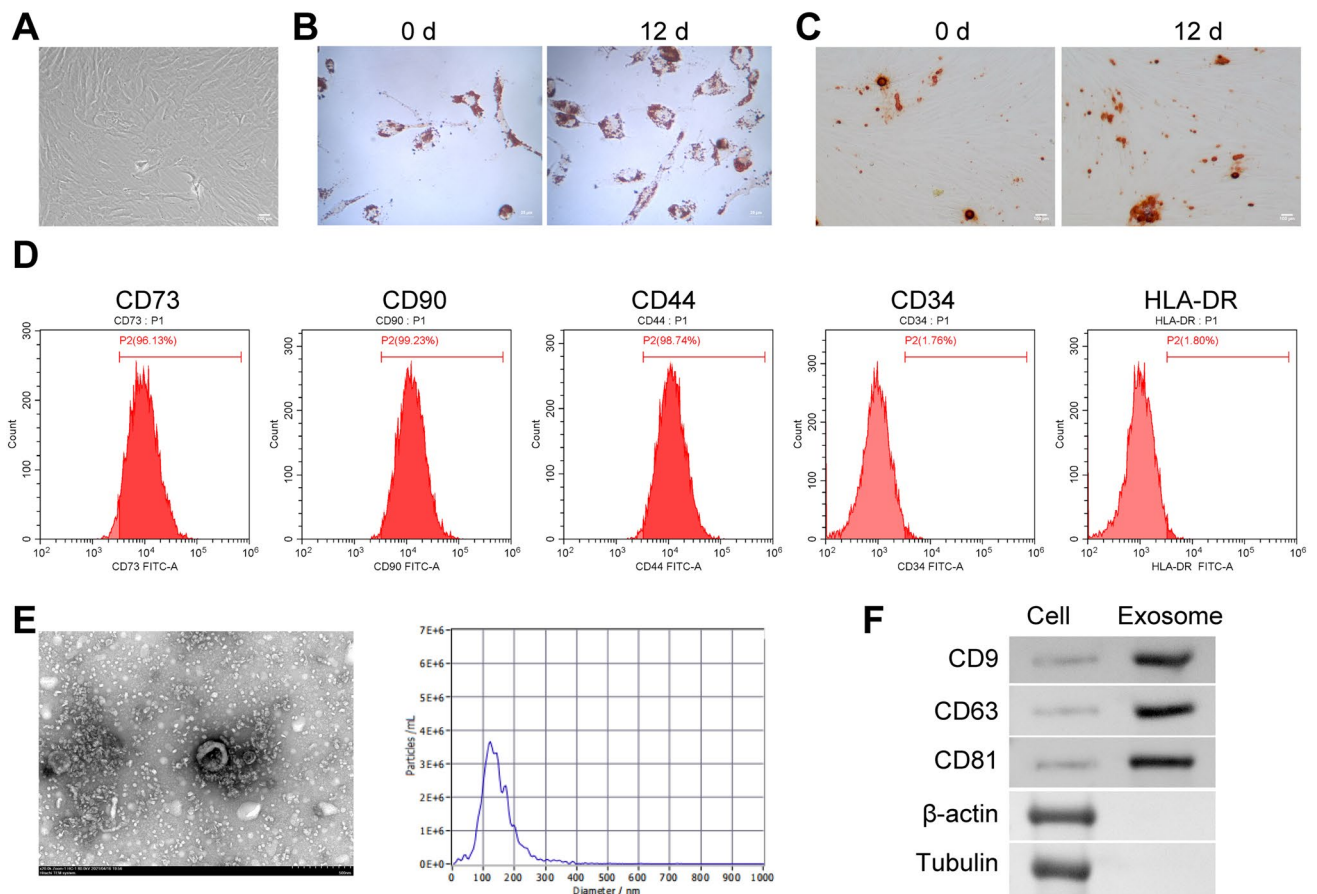


Fig. 1 Culture and identification of ASC and ASC-exos. **A** Cell morphology observation of ASC. **B**, **C** Oil red O staining and alizarin red staining was applied to observe the lipogenic and osteogenic differentiation ASC. **D** The expression of the CD73, CD90, CD44, CD34,

and HLA-DR markers in ASC was detected by flow cytometry. **E** Electron microscope was applied to observe exosomes. **F** The expressions of CD9, CD63, CD81, β -actin and Tubulin were detected by western blot. * $P < 0.05$ versus 0 d

Data statistics and analysis

Graphpad Prism 8.0 statistical software was used for statistical analysis of data in this study. The measurement data were expressed as mean \pm standard deviation. First, the data are tested for normality and homogeneity of variance. The test conformed to normal distribution and homogeneity of variance. Unpaired t-test was used between groups. One-way ANOVA analysis or analysis of variance of repeated measurement data were used for comparison among multiple groups. Tukey's was used for the post test. $P < 0.05$ means the difference was statistically significant.

Results

Culture and identification of ASC and ASC-exos

As the incubation time increases, ASC gradually becomes homogeneous, forming a monolayer of adherent cells, and

displays typical fibroblast-like morphology (Fig. 1A). The third generation of ASCs is collected for pluripotency identification. After 3 weeks of incubation in adipogenic differentiation medium, most cells exhibit characteristics of adipocytes stained with oil red O (Fig. 1B). Similarly, after incubation in osteogenic differentiation medium, most cells show differentiation into osteoblasts stained with alizarin red (Fig. 1C). In addition, flow cytometry characterization reveals that ASCs are strongly positive for CD73 (96.13%), CD90 (99.23%), and CD44 (98.74%) but negative for CD34 (1.74%) and HLA-DR (1.80%) (Fig. 1D). Electron microscopy showed that the diameter of exosomes secreted by ASC was about 100–140 nm (Fig. 1E). The CD9, CD63 and CD81 proteins were highly expressed, while β -actin and Tubulin proteins were not expressed in exosomes (Fig. 1F), which proved that we successfully isolated ASC-exos. The above results proved that we have successfully obtained human ASC and ASC-exos.

ASC-exos influenced CD4⁺T cell differentiation

The PKH26 expression was localized in CD4⁺T cells, indicating that CD4⁺T cells were able to take up ASC-exos (Fig. 2A). ASC-exos inhibited Th1 and Th17 differentiation and promoted Treg differentiation of CD4⁺T cells in a dose-dependent manner (Fig. 2B-D, Supplementary Fig. 1). In addition, ASC-exos inhibited the IFN- γ and IL17 expression and promoted the FoxP3 expression in CD4⁺T cells (Fig. 2E). ASC-exos downregulated the mRNA ratio of IFN- γ /FoxP3 and IL17/FoxP3 in CD4⁺T cells (Fig. 2E). These results demonstrated that ASC-exos influenced the differentiation of Treg/Th17 cells in CD4⁺T cells.

ASC-exos influenced macrophage differentiation from CD14⁺ monocytes

IF staining showed that macrophages could ingest ASC-exos (Fig. 3A). ASC-exos inhibited M1 differentiation and promoted M2 differentiation of macrophages in a dose-dependent manner (Fig. 3B). ASC-exos increased the CD206(+) CD86(+) macrophages (Fig. 3C). In addition, ASC-exos promoted the Arg-1 and CD163 expression and inhibited the TNF- α and iNOS expression in macrophages (Fig. 3E). ASC-exos upregulated the mRNA ratio of Arg-1/iNOS in macrophages (Fig. 3D). These results demonstrated that ASC-exos promoted M2-type differentiation of macrophages.

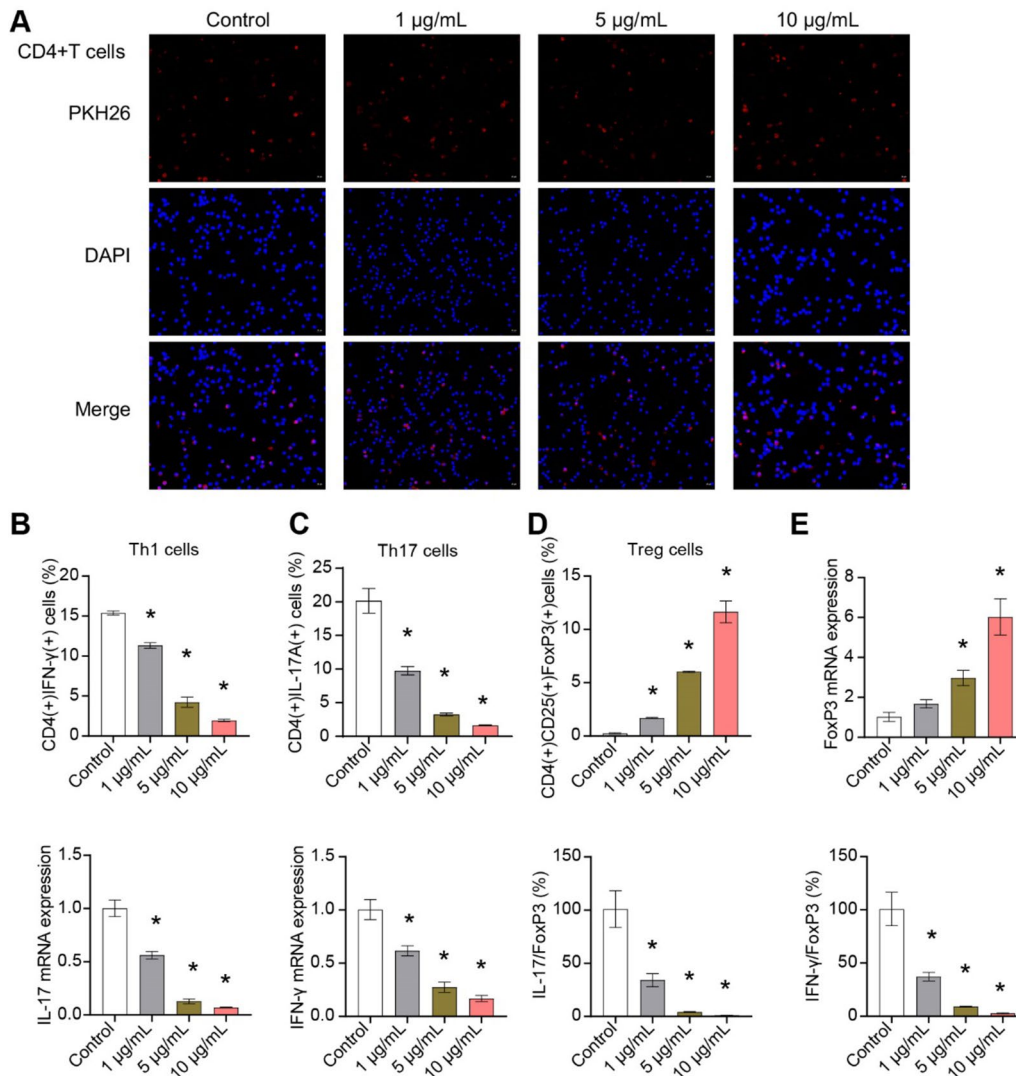


Fig. 2 ASC-exos affected the Treg/Th17 cell differentiation in CD4⁺T cells. **A** Cellular localization of PKH26 was determined by exosomes uptake test. **B–D** Flow cytometry was used to detect the

proportion of Th1, Th17 and Treg cells. **E** The expressions of IFN- γ , IL-17 and FoxP3 genes were detected by qRT-PCR. **P* < 0.05 versus Control

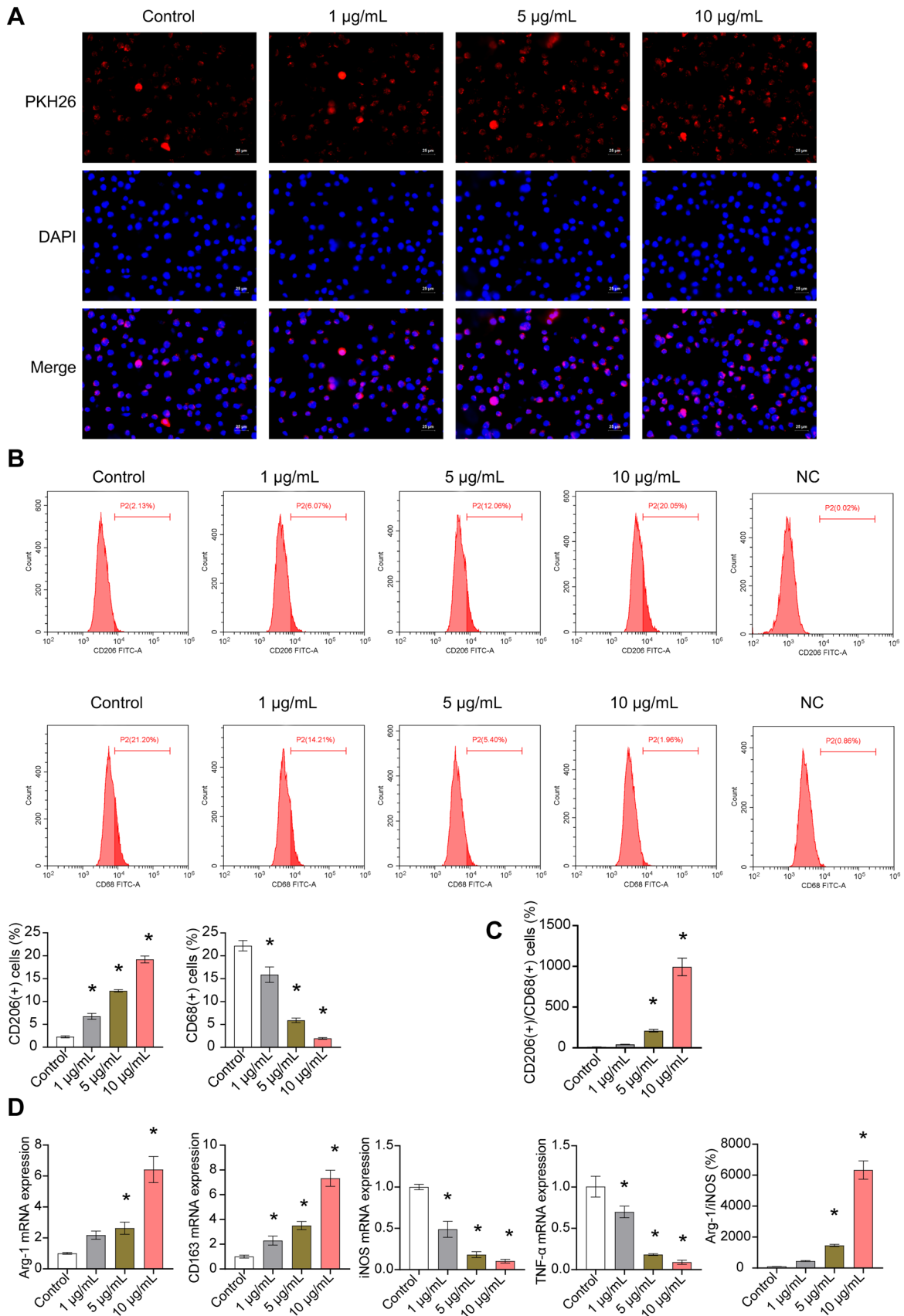


Fig. 3 ASC-exos influenced macrophage differentiation. **A** Cellular localization of PKH26 was determined by exosomes uptake test. **B–C** The proportion of M1 and M2 cells were determined by flow cytometry. **D** The expressions of Arg-1, CD163, TNF- α and iNOS were detected by qRT-PCR. * $P < 0.05$ versus Control

ASC-exos affected the characterization of MCF-7 cells

IF showed that MCF-7 cells could take up exosomes from ASC (Fig. 4A). ASC-exos promoted the proliferation, migration, and invasion of MCF-7 cells in a dose-dependent manner (Fig. 4B–D, Supplementary Fig. 2A,B). In addition, ASC-exos inhibited apoptosis of MCF-7 cells (Fig. 4E, Supplementary Fig. 2C). ASC-exos promoted the expression of Bcl-2, ERBB2, Ki67 and inhibited the expression of Bax in MCF-7 cells (Fig. 4F–G). These results demonstrated that ASC-exos promoted the basic characterization of MCF-7 cells.

ASC-exos promoted the formation of breast cancer in nude mice

Nude mouse tumorigenesis showed that ASC-exos promoted tumorigenesis of breast cancer cells (Fig. 5A, B). ASC-exos significantly increased the tumorigenic volume and weight of MCF-7 cells (Fig. 5B, C). HE staining showed that compared to the control group, there were more red blood cells and tumor cells in the exosome group (Fig. 5D). IHC analysis found that ASC-exos increased the Ki67 expression in tumor tissues (Fig. 5E). All the results proved that ASC-exos promoted the development of breast cancer tumors.

ASC-exos influenced tumor microenvironment immunity of breast cancer

ASC-exos inhibited the differentiation of CD8, Th1 and Th17 cells, and promoted the differentiation of Treg cells in tumor tissues (Fig. 6A, B, Supplementary Fig. 3). ASC-exos promoted the FxoP3 expression and inhibited the IFN- γ and IL-17 expression in tumor tissues (Fig. 6C, D). IF further confirmed that ASC-exos promoted the FxoP3 expression in tumor tissue (Fig. 6E). ASC-exos influenced the tumor microenvironment immunity of breast cancer.

ASC-exos influenced tumor macrophage differentiation in breast cancer

ASC-exos promoted M2-polarization and inhibited M1-polarization of macrophages in breast cancer tumor tissue, thereby worsening the tumor (Fig. 7A, B). ASC-exos increased the CD206(+)/CD86(+) macrophages (Fig. 7C). In addition, ASC-exos promoted the Arg-1 and CD163

expression and inhibited the TNF- α expression and iNOS (Fig. 7D–G). ASC-exos upregulated the ratio of Arg-1/iNOS expression in macrophages (Fig. 7E and G). These results demonstrated that ASC-exos promoted the polarization of M2-type macrophages in breast cancer and worsen the tumor.

ASC-exos influenced T cell function in breast cancer

We used RNAseq to analyze the changes of RNA expression profile and function in breast cancer tumor tissues before and after exosome intervention. PCA analysis showed that the samples from control group and exosome group showed discrete distribution, with crossover and deviation (Fig. 8A). Volcano map proved that 17 genes were higher and 22 genes were lower under the ASC-exos treatment (Fig. 8B). Heatmap showed variations in the abundance of 39 differential genes (Fig. 8C). KEGG functional enrichment analysis showed that the Human T-cell leukemia virus 1 infection pathway was significantly enriched in exosome group (Fig. 8D). The TOX, CD4, and LYZ1 genes were higher, and the CSF3 and Serpinb2 genes were lower in exosome group, which was consistent with sequencing results (Fig. 8E). These results proved that ASC-exos affected T cell function in breast cancer tumor tissues.

Discussion

The tumor microenvironment plays an important role in inducing cancer cells to enter dormancy and participate in reversible epithelial-mesenchymal transition (EMT) to an aggressive phenotype that leads to cancer-related death in patients [21]. Direct cell-to-cell contact between cancer cells and ASC via exosomes vesicle exchange caused breast cancer cells to exhibit changes toward a more malignant phenotype [22, 23]. All these were associated with higher rates of metastasis and a worsening prognosis [22]. Exosomes secreted by adipose tissue-derived MSCs could induce apoptosis and inhibit metastasis of breast cancer cells by repairing miR-145 [24]. Adipose-derived MSC-exosomes could deliver miR-1236 to increase the sensitivity of breast cancer cells to DDP by participating in SLC9A1 downregulation and Wnt/ β -catenin inactivation [25]. Adipose-derived MSC-exosomes were successfully isolated and internalized by MDA-MB-231 cells, and miR-381 mimics were effectively delivered to MDA-MB-231 cells by the MSC-exosomes [26]. Our in vitro and in vivo studies confirmed that ASC-exos promoted the migration, proliferation, and invasion of MCF-7 cells, inhibited apoptosis in a dose-dependent manner. These studies confirmed that ASC-exos promoted malignant characterization of breast cancer cells.

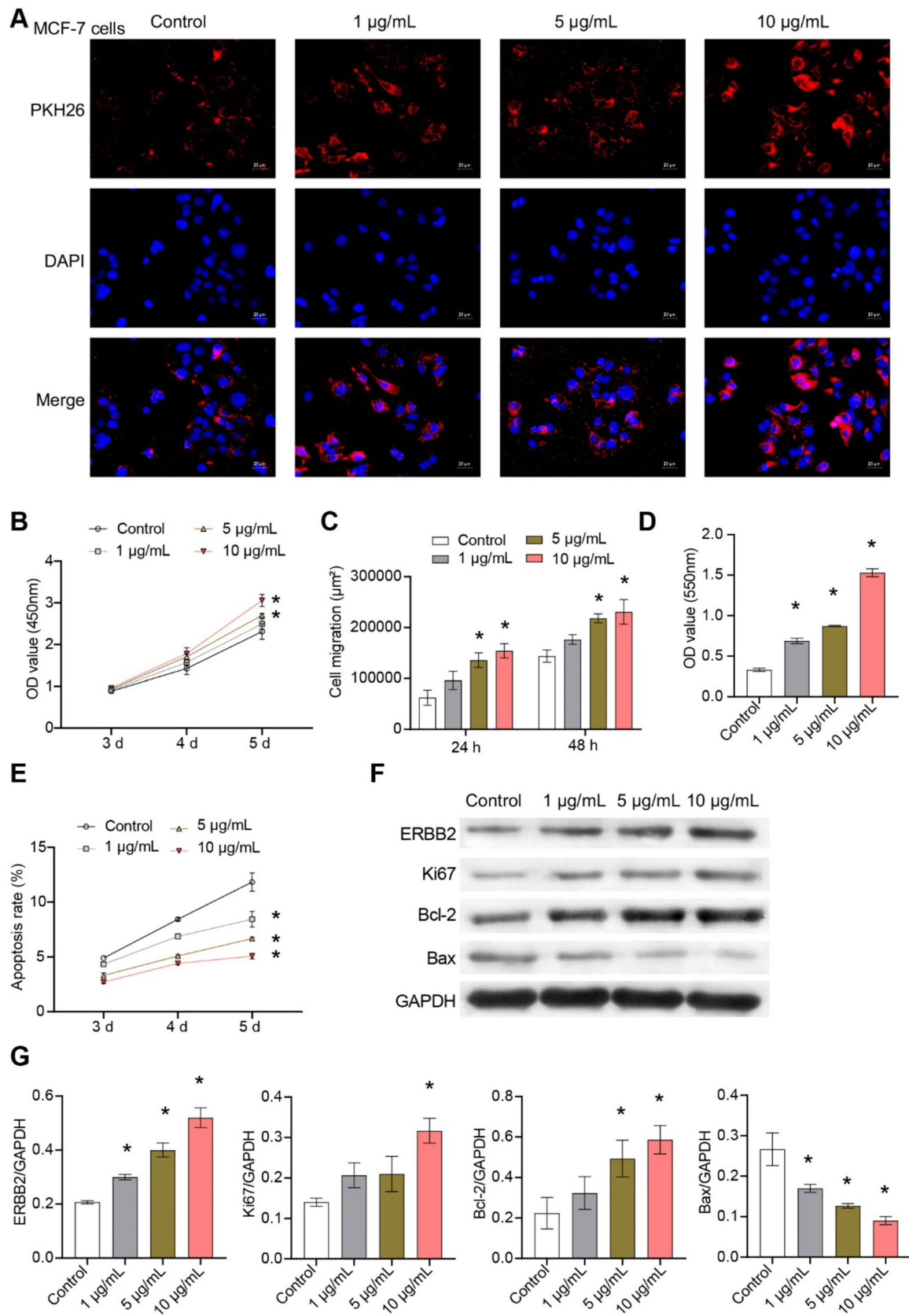


Fig. 4 ASC-exos affected the basic characterization of MCF-7 cells. **A** Cellular localization of PKH26 was determined by exosomes uptake test. **B** Cell proliferation was detected by CCK8. **C** Cell migration was detected by scratch assay. **D** Transwell was used to detect cell invasion. **E** Apoptosis was detected by flow cytometry. **F–G** The expressions of Bcl-2, Bax, ERBB2 and Ki67 were detected by western blot. * $P < 0.05$ versus Control

In addition to its direct effect on tumor cells, obesity also systematically provided a prerequisite for future metastasis of the tumor microenvironment by promoting

the formation of pro-inflammatory niches [27]. Exosomes of adipose-derived MSC ameliorated experimental colitis by inhibiting Th1/Th17 cells and macrophages and reducing the pro-inflammatory cytokines level [28]. ASC-exos promoted angiogenesis and cancer cell migration and have neuroprotective and nerve regeneration properties [29]. The delivery of miR-424-5p targeting PD-L1 by EVs derived from adipose tissue MSC promoted proinflammatory effects [30]. Adipose tissue-derived MSC-exosomes with miR-10a promoted Th17 and Tregs responses while reduced Th1

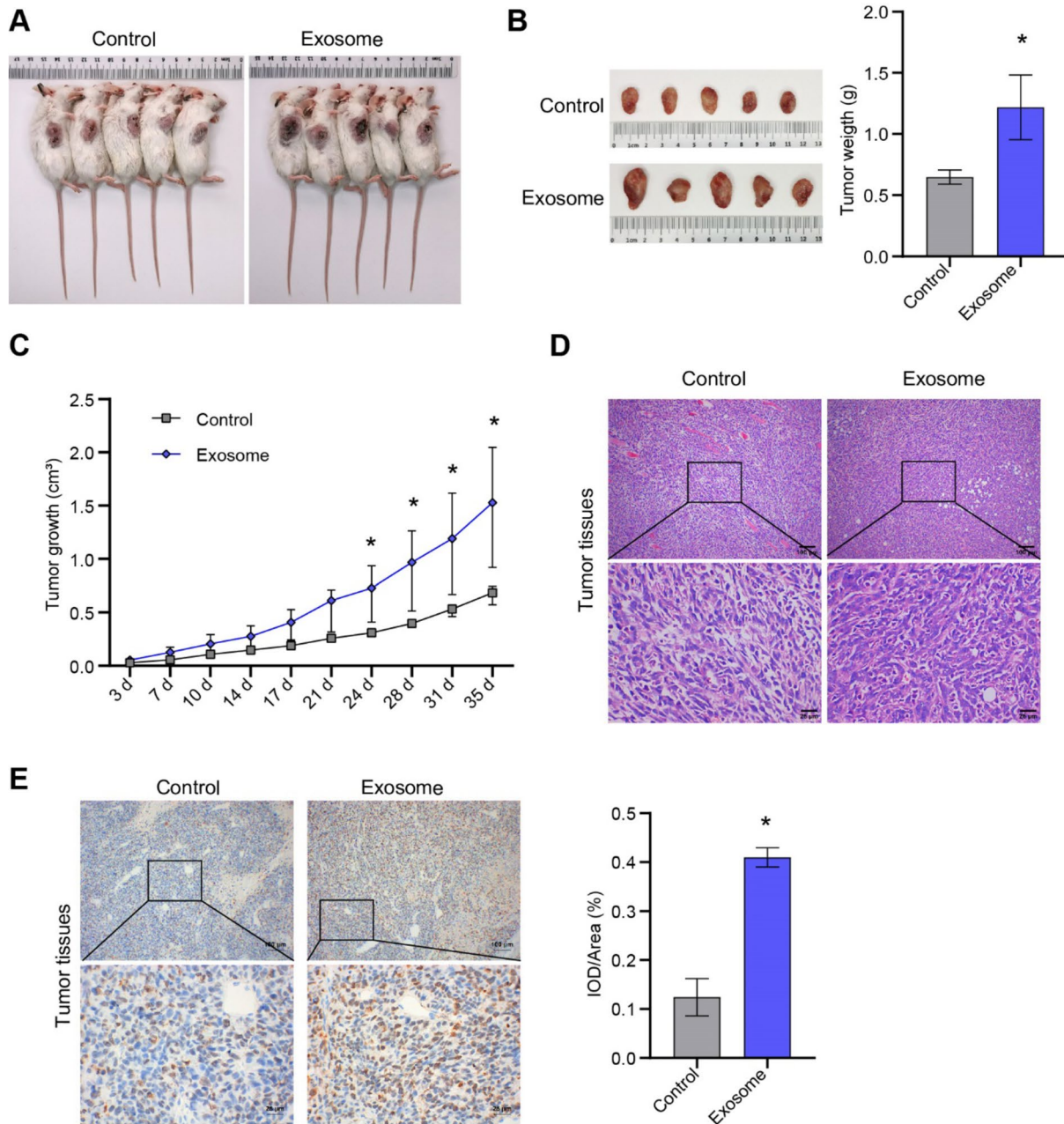


Fig. 5 ASC-exos promoted breast cancer formation. **A** Tumor formation was observed in nude mice. **B** The observation and weight analysis of tumor tissues. **C** Tumor volume cure. **D** HE staining was

applied to observe the pathological changes of tumor tissue. **E** The expression of Ki67 was observed by IHC. * $P < 0.05$ versus Control

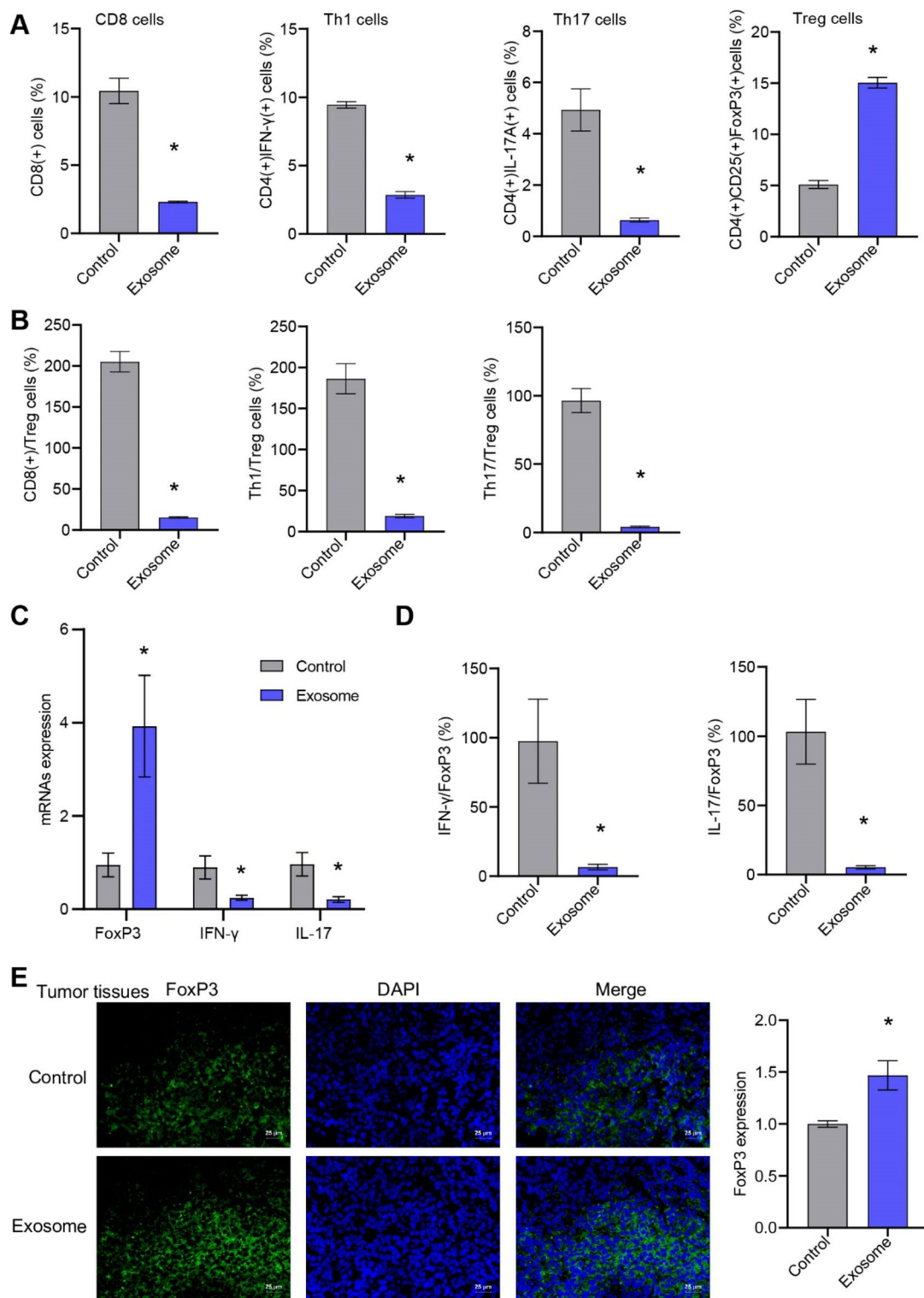


Fig. 6 ASC-exos influenced tumor microenvironment immunity of breast cancer. **A, B** The proportion of CD8, Th1, Th17, and Treg cells in tumor tissue were tested by flow cytometry. **C, D** The expression of

FoxP3, IFN-γ and IL-17 in tumor tissues was detected by qRT-PCR. **E** The expression of FoxP3 was detected by IF (25 μm). **P* < 0.05 versus Control

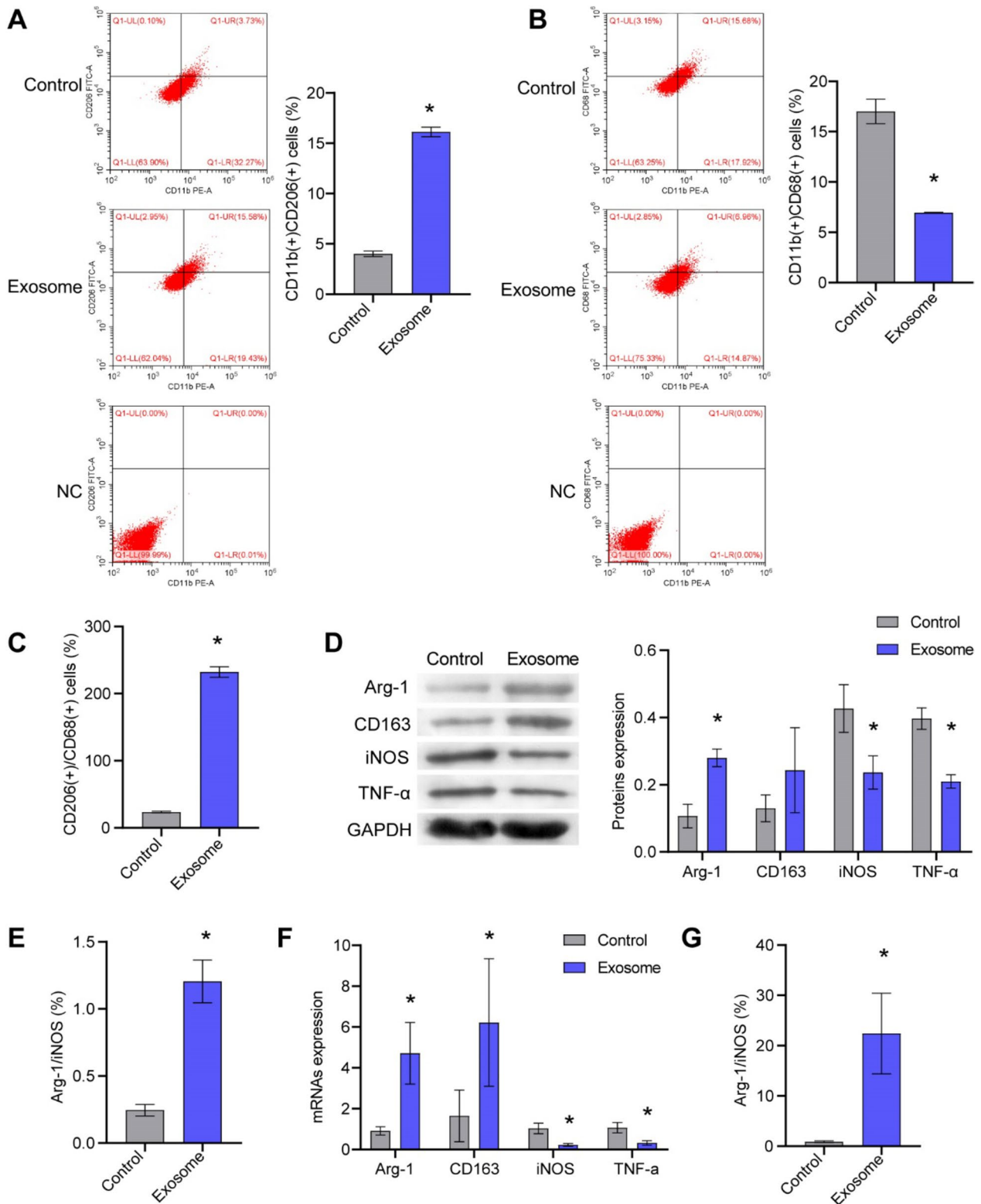


Fig. 7 ASC-exos influenced tumor macrophage differentiation in breast cancer. **A–C** The proportion of M1 and M2 macrophages in breast cancer was analyzed by flow cytometry. **D–G** The expressions

of Arg-1, CD163, TNF- α and iNOS were tested by qRT-PCR and western blot. * $P < 0.05$ versus Control

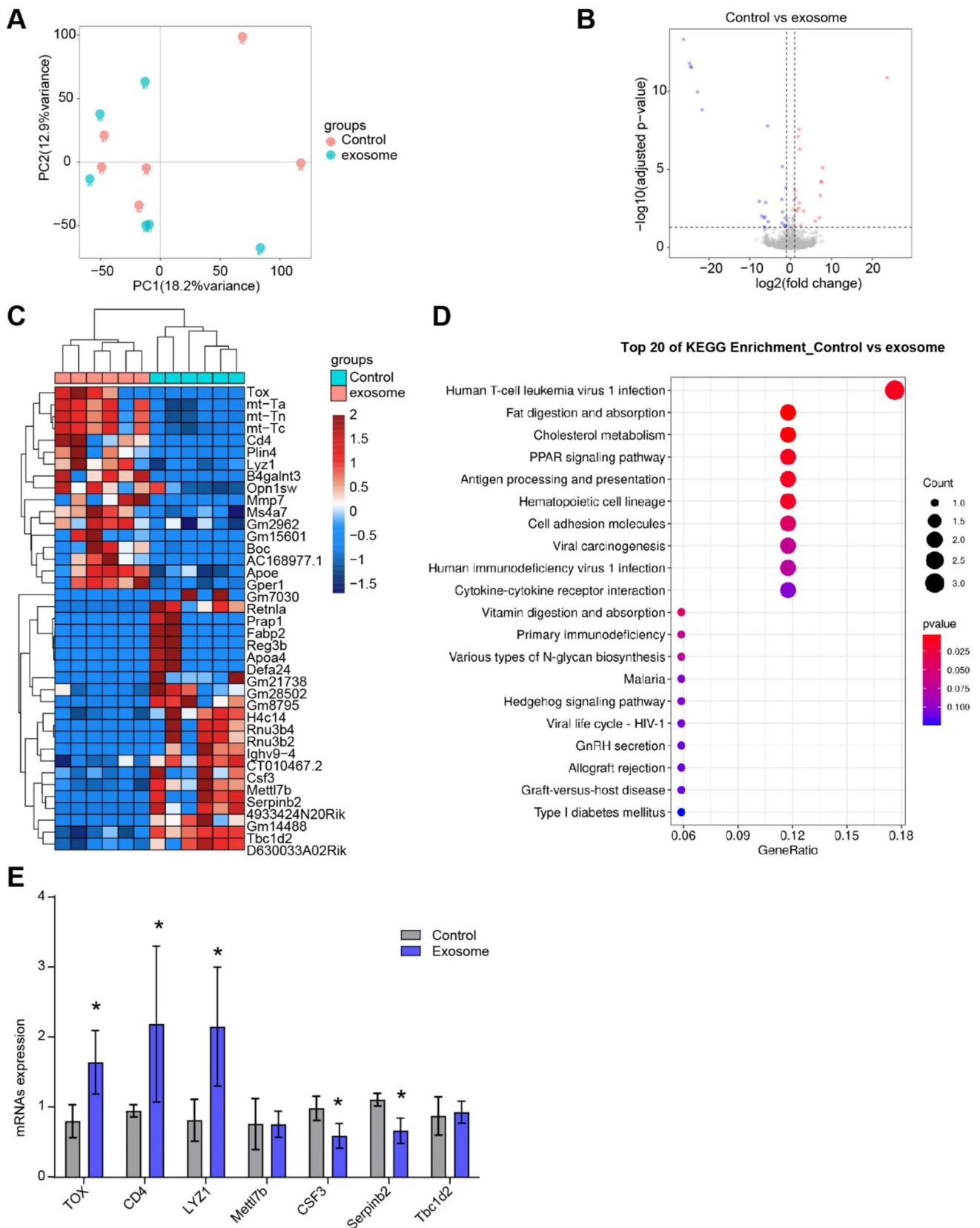


Fig. 8 ASC-exos influenced T cell function in breast cancer tumor tissues. **A** PCA analysis. **B** volcano plot. **C** Heatmap showed the gene abundance. **D** KEGG was applied to predict the function of differen-

tial genes. **E** qRT-PCR was applied to verify the differential genes expression in breast cancer tissues. **P* < 0.05 versus Control

responses [31]. Our studies confirmed that ASC-exos inhibited Th1 and Th17 differentiation of CD4⁺T cells, promoted Treg differentiation, and inhibited M1/M2 differentiation of macrophages, which were partly consistent with the above studies.

ASC have been shown to favor tumor progression in several experimental cancer models, playing a central role in regulating tumor aggressions and metastatic potential through a variety of mechanisms, such as paracrine release of exosomes containing cancer-promoting molecules and induction of EMT [32]. Tumor-derived exosomes induced myofibroblasts phenotype and function in ASC through a SMAD-mediated signaling pathway, thereby promoting tumor cell progression and malignancy [33]. MSC-exosomes promoted the migration of breast cancer cell line MCF7 and were associated with WNT signaling pathway activation [34]. Small extracellular vesicles from immune cells and other donor cells can be engineered to provide better targeting and biological effects [35]. All these studies were consistent with our study, which confirmed that ASC-exos influenced the tumor microenvironment immunity of breast cancer to promote the malignant characterization of breast cancer, provided new evidence for ASC-exos.

However, conflicting evidence has emerged regarding the safety of ASC applications in recent years [36]. Extracellular vesicles regulate a variety of cancer-related processes by transmitting homologous and heterologous cell communication cues [37]. The intervention of exosomes from osteoblast ASC in cancer stem cells could significantly reduce the expression of ATP-binding box (ABC) transporters, breast cancer gene family (BCRA1 and BCRA2), ErbB gene family and other drug-resistant genes, helping to overcome the treatment resistance [38]. In addition, drug delivery via exosome could reduce the cell viability of MCF7 cell and without any significant cytotoxicity to normal L929 cell, which has great potential for clinical application [39]. ASC conditioned media could induce selective stress by increasing cell proliferation, resulting in a more aggressive phenotype in MCF-7 and MDA-MB-231 cells [40]. Our results confirmed that ASC-exos promoted the TOX, CD4, and LYZ1 expression and inhibited the Mettl7b and Serpinb2 expression in breast cancer tumors, which were significantly enriched in the Human T-cell leukemia virus 1 infection pathway. Therefore, ASC exosomes promote the development of breast cancer by regulating the expression of RNA expression profiles in breast cancer tissues.

This study focuses on the analysis of the effects of ASC-derived exosomes on the malignant characteristics and tumor formation of breast cancer cells. In addition, ASC-exosomes are rich in proteins, lipids, and nucleic acids, serving as crucial mediators in key biological processes in cells and tissues

through intracellular signaling mechanisms [41]. Given the limitations of proteomics technology and experimental funding, we took a different approach and used RNA-seq to explore the effects of ASC-derived exosomes intervention on the RNA expression profile in tumor tissues. But the specific contents of ASC-derived exosomes were not clearly analyzed. This limitation of our study needs to be further explored in future research. Further exploration of the potential functions of proteins, lipids, or nucleic acids in ASC-derived exosomes may provide new directions for our next study, but some potential technical issues still need to be addressed. However, our study does provide initial evidence that ASC-derived exosomes promote the malignant characteristics of breast cancer and play a role in regulating the tumor microenvironment immune response, which highlights the significance of this research.

In conclusion, ASC-exos promoted breast cancer characterization and tumor microenvironment immunosuppression by regulating macrophage typing and T cell differentiation-related functional gene expression.

Supplementary Information The online version contains supplementary material available at <https://doi.org/10.1007/s00262-023-03584-3>.

Author contributions QZ contributed to conceptualization, data curation, investigation, methodology, validation, and writing of the original draft. YC and JY contributed to conceptualization, formal analysis, investigation, software, and validation. YH contributed to conceptualization, funding acquisition, project administration, supervision, and review.

Funding This work was supported by Natural Science Foundation of Hunan Province (No.2022JJ30994).

Data availability The data that support the findings of this study are available from the corresponding author upon reasonable request.

Declarations

Conflicts of interest None.

Ethics approval and consent to participate The study was approved by the Human Research Ethics Committee of Xiangya Hospital, Central South University (AF/SQ 2022090918). The research was conducted according to the World Medical Association Declaration of Helsinki. All the information about the study will be fully explained to the subjects by the researchers. All the participants provided informed consent before sampling. This study was approved by the Animal Ethics Committee of Xiangya Hospital, Central South University (AF/SQ 2022090918). All experimental procedures were conducted in accordance with institutional guidelines for the use of experimental animals.

Open Access This article is licensed under a Creative Commons Attribution 4.0 International License, which permits use, sharing, adaptation, distribution and reproduction in any medium or format, as long as you give appropriate credit to the original author(s) and the source, provide a link to the Creative Commons licence, and indicate if changes were made. The images or other third party material in this article are included in the article's Creative Commons licence, unless indicated

otherwise in a credit line to the material. If material is not included in the article's Creative Commons licence and your intended use is not permitted by statutory regulation or exceeds the permitted use, you will need to obtain permission directly from the copyright holder. To view a copy of this licence, visit <http://creativecommons.org/licenses/by/4.0/>.

References

- Katsura C, Ogunmwoyoni I, Kankam HK, Saha S (2022) Breast cancer: presentation, investigation and management. *Br J Hosp Med* 83(2):1–7. <https://doi.org/10.12968/hmed.2021.0459>
- Dieci MV, Miglietta F, Guarneri V (2021) Immune infiltrates in breast cancer: recent updates and clinical implications. *Cells* 10(2):223. <https://doi.org/10.3390/cells10020223>
- Bhaskaran K, Douglas I, Forbes H, dos Santos-Silva I, Leon DA, Smeeth L (2014) Body-mass index and risk of 22 specific cancers: a population-based cohort study of 5.24 million UK adults. *Lancet* 384(9945):755–765. [https://doi.org/10.1016/s0140-6736\(14\)60892-8](https://doi.org/10.1016/s0140-6736(14)60892-8)
- Donohoe CL, Lysaght J, O'Sullivan J, Reynolds JV (2017) Emerging concepts linking obesity with the hallmarks of cancer. *Trends Endocrinol Metab* 28(1):46–62. <https://doi.org/10.1016/j.tem.2016.08.004>
- Picon-Ruiz M, Marchal JA, Slingerland JM (2020) Obtaining human breast adipose cells for breast cancer cell co-culture studies. *STAR Protoc* 1(3):100197. <https://doi.org/10.1016/j.xpro.2020.100197>
- Li P, Lu M, Shi J, Gong Z, Hua L, Li Q et al (2020) Lung mesenchymal cells elicit lipid storage in neutrophils that fuel breast cancer lung metastasis. *Nat Immunol* 21(11):1444–1455. <https://doi.org/10.1038/s41590-020-0783-5>
- Banani MA, Rahmatullah M, Farhan N, Hancox Z, Yousaf S, Arabpour Z et al (2021) Adipose tissue-derived mesenchymal stem cells for breast tissue regeneration. *Regen Med* 16(1):47–70. <https://doi.org/10.2217/rme-2020-0045>
- Bielli A, Scioli MG, Gentile P, Agostinelli S, Tarquini C, Cervelli V et al (2014) Adult adipose-derived stem cells and breast cancer: a controversial relationship. *Springerplus* 3:345. <https://doi.org/10.1186/2193-1801-3-345>
- Schweizer R, Tsuji W, Gorantla VS, Marra KG, Rubin JP, Plock JA (2015) The role of adipose-derived stem cells in breast cancer progression and metastasis. *Stem Cells Int* 2015:120949. <https://doi.org/10.1155/2015/120949>
- Quail DF, Dannenberg AJ (2019) The obese adipose tissue microenvironment in cancer development and progression. *Nat Rev Endocrinol* 15(3):139–154. <https://doi.org/10.1038/s41574-018-0126-x>
- Ritter A, Kreis NN, Hoock SC, Solbach C, Louwen F, Yuan J (2022) Adipose tissue-derived mesenchymal stromal/stem cells, obesity and the tumor microenvironment of breast cancer. *Cancers (Basel)* 14(16):3908. <https://doi.org/10.3390/cancers14163908>
- Xiong M, Zhang Q, Hu W, Zhao C, Lv W, Yi Y et al (2020) Exosomes from adipose-derived stem cells: The emerging roles and applications in tissue regeneration of plastic and cosmetic surgery. *Front Cell Dev Biol* 8:574223. <https://doi.org/10.3389/fcell.2020.574223>
- Shukla L, Yuan Y, Shayan R, Greening DW, Karnezis T (2020) Fat therapeutics: The clinical capacity of adipose-derived stem cells and exosomes for human disease and tissue regeneration. *Front Pharmacol* 11:158. <https://doi.org/10.3389/fphar.2020.00158>
- Blazquez R, Sanchez-Margallo FM, de la Rosa O, Dalemans W, Álvarez V, Tarazona R et al (2014) Immunomodulatory potential of human adipose mesenchymal stem cells derived exosomes on in vitro stimulated T cells. *Front Immunol* 5:556
- Li X, Liu L, Yang J, Yu Y, Chai J, Wang L et al (2016) Exosome derived from human umbilical cord mesenchymal stem cell mediates MiR-181c attenuating burn-induced excessive inflammation. *EBioMedicine* 8:72–82
- Heo JS, Choi Y, Kim HO (2019) Adipose-derived mesenchymal stem cells promote M2 macrophage phenotype through exosomes. *Stem Cells Int*. 2019
- Théry C, Duban L, Segura E, Véron P, Lantz O, Amigorena S (2002) Indirect activation of naïve CD4+ T cells by dendritic cell-derived exosomes. *Nat Immunol* 3(12):1156–1162
- Jiang L, Zhang S, Hu H, Yang J, Wang X, Ma Y et al (2019) Exosomes derived from human umbilical cord mesenchymal stem cells alleviate acute liver failure by reducing the activity of the NLRP3 inflammasome in macrophages. *Biochem Biophys Res Commun* 508(3):735–741
- Zhong X, Zhang W, Sun T (2019) DDR1 promotes breast tumor growth by suppressing antitumor immunity. *Oncol Rep* 42(6):2844–2854. <https://doi.org/10.3892/or.2019.7338>
- Yang S-S, Ma S, Dou H, Liu F, Zhang S-Y, Jiang C et al (2020) Breast cancer-derived exosomes regulate cell invasion and metastasis in breast cancer via miR-146a to activate cancer associated fibroblasts in tumor microenvironment. *Exp Cell Res* 391(2):111983
- Mohd Ali N, Yeap SK, Ho WY, Boo L, Ky H, Satharasinghe DA et al (2020) Adipose MSCs suppress MCF7 and MDA-MB-231 breast cancer metastasis and EMT pathways leading to dormancy via exosomal-miRNAs following co-culture interaction. *Pharmaceuticals (Basel)* 14(1):8. <https://doi.org/10.3390/ph14010008>
- Kuhbier JW, Bucan V, Reimers K, Strauss S, Lazaridis A, Jahn S et al (2014) Observed changes in the morphology and phenotype of breast cancer cells in direct co-culture with adipose-derived stem cells. *Plast Reconstr Surg* 134(3):414–423. <https://doi.org/10.1097/prs.0000000000000525>
- Buzas EI (2023) The roles of extracellular vesicles in the immune system. *Nat Rev Immunol* 23(4):236–250. <https://doi.org/10.1038/s41577-022-00763-8>
- Sheykhasan M, Kalhor N, Shekholeslami A, Dolati M, Amini E, Fazaeli H (2021) Exosomes of mesenchymal stem cells as a proper vehicle for transfecting miR-145 into the breast cancer cell line and its effect on metastasis. *Biomed Res Int* 2021:5516078. <https://doi.org/10.1155/2021/5516078>
- Jia Z, Zhu H, Sun H, Hua Y, Zhang G, Jiang J et al (2020) Adipose mesenchymal stem cell-derived exosomal microRNA-1236 reduces resistance of breast cancer cells to cisplatin by suppressing SLC9A1 and the Wnt/ β -catenin signaling. *Cancer Manag Res* 12:8733–8744. <https://doi.org/10.2147/cmar.S270200>
- Shojaei S, Hashemi SM, Ghanbarian H, Sharifi K, Salehi M, Mohammadi-Yeganeh S (2021) Delivery of miR-381-3p mimic by mesenchymal stem cell-derived exosomes inhibits triple negative breast cancer aggressiveness; an in vitro study. *Stem Cell Rev Rep* 17(3):1027–1038. <https://doi.org/10.1007/s12015-020-10089-4>
- Robado de Lope L, Alcázar OL, Amor López A, Hergueta-Redondo M, Peinado H (2018) Tumour-adipose tissue crosstalk: fuelling tumour metastasis by extracellular vesicles. *Philos Trans R Soc Lond B Biol Sci* 373(1737):20160485. <https://doi.org/10.1098/rstb.2016.0485>
- Guo G, Tan Z, Liu Y, Shi F, She J (2022) The therapeutic potential of stem cell-derived exosomes in the ulcerative colitis and colorectal cancer. *Stem Cell Res Ther* 13(1):138. <https://doi.org/10.1186/s13287-022-02811-5>
- Gao X, Salomon C, Freeman DJ (2017) Extracellular vesicles from adipose tissue—a potential role in obesity and type 2 diabetes? *Front Endocrinol (Lausanne)* 8:202. <https://doi.org/10.3389/fendo.2017.00202>

30. Zhou Y, Yamamoto Y, Takeshita F, Yamamoto T, Xiao Z, Ochiya T (2021) Delivery of miR-424–5p via extracellular vesicles promotes the apoptosis of MDA-MB-231 TNBC cells in the tumor microenvironment. *Int J Mol Sci* 22(2):844. <https://doi.org/10.3390/ijms22020844>
31. Bolandi Z, Mokhberian N, Eftekhary M, Sharifi K, Soudi S, Ghanbarian H et al (2020) Adipose derived mesenchymal stem cell exosomes loaded with miR-10a promote the differentiation of Th17 and Treg from naive CD4(+) T cell. *Life Sci* 259:118218. <https://doi.org/10.1016/j.lfs.2020.118218>
32. Gentile P, Garcovich S (2019) Concise review: adipose-derived stem cells (ASCs) and adipocyte-secreted exosomal microRNA (A-SE-miR) modulate cancer growth and proMote wound repair. *J Clin Med* 8(6):855. <https://doi.org/10.3390/jcm8060855>
33. Cho JA, Park H, Lim EH, Lee KW (2012) Exosomes from breast cancer cells can convert adipose tissue-derived mesenchymal stem cells into myofibroblast-like cells. *Int J Oncol* 40(1):130–138. <https://doi.org/10.3892/ijo.2011.1193>
34. Lin R, Wang S, Zhao RC (2013) Exosomes from human adipose-derived mesenchymal stem cells promote migration through Wnt signaling pathway in a breast cancer cell model. *Mol Cell Biochem* 383(1–2):13–20. <https://doi.org/10.1007/s11010-013-1746-z>
35. Qian K, Fu W, Li T, Zhao J, Lei C, Hu S (2022) The roles of small extracellular vesicles in cancer and immune regulation and translational potential in cancer therapy. *J Exp Clin Cancer Res* 41(1):286. <https://doi.org/10.1186/s13046-022-02492-1>
36. Guillaume VGJ, Ruhl T, Boos AM, Beier JP (2022) The cross-talk between adipose-derived stem or stromal cells (ASC) and cancer cells and ASC-mediated effects on cancer formation and progression-ASCs: safety hazard or harmless source of tropism? *Stem Cells Transl Med* 11(4):394–406. <https://doi.org/10.1093/scitlm/szac002>
37. Beltraminelli T, Perez CR, De Palma M (2021) Disentangling the complexity of tumor-derived extracellular vesicles. *Cell Rep* 35(1):108960. <https://doi.org/10.1016/j.celrep.2021.108960>
38. Lee KS, Choi JS, Cho YW (2019) Reprogramming of cancer stem cells into non-tumorigenic cells using stem cell exosomes for cancer therapy. *Biochem Biophys Res Commun* 512(3):511–516. <https://doi.org/10.1016/j.bbrc.2019.03.072>
39. Ebrahimiyan M, Hashemi M, Etemad L, Salmasi Z (2022) Thymoquinone-loaded mesenchymal stem cell-derived exosome as an efficient nano-system against breast cancer cells. *Iran J Basic Med Sci* 25(6):723–731. <https://doi.org/10.22038/ijbms.2022.64092.14116>
40. de Miranda MC, Ferreira ADF, de Melo MIA, Kunrath-Lima M, Goes AM, Rodrigues MA et al (2021) Adipose-derived stem/stromal cell secretome modulates breast cancer cell proliferation and differentiation state towards aggressiveness. *Biochimie* 191:69–77. <https://doi.org/10.1016/j.biochi.2021.08.010>
41. Lee JH, Won YJ, Kim H, Choi M, Lee E, Ryoou B et al (2023) Adipose tissue-derived mesenchymal stem cell-derived exosomes promote wound healing and tissue regeneration. *Int J Mol Sci* 24(13):10434. <https://doi.org/10.3390/ijms241310434>

Publisher's Note Springer Nature remains neutral with regard to jurisdictional claims in published maps and institutional affiliations.